Structure, Synthesis, and Activity of Dermaseptin *b*, a Novel Vertebrate Defensive Peptide from Frog Skin: Relationship with Adenoregulin

Amram Mor, Mohamed Amiche, and Pierre Nicolas*

Laboratoire de Bioactivation des Peptides, Institut Jacques Monod, CRNS-Université Paris 7, 2 place Jussieu, 75251 Paris Cedex 05, France

Received November 29, 1993; Revised Manuscript Received March 10, 1994®

ABSTRACT: A novel antimicrobial peptide, designated dermaseptin *b*, was isolated from the skin of the arboreal frog *Phyllomedusa bicolor*. This 27-residue peptide amide is basic, containing 3 lysine residues that punctuate an alternating hydrophobic and hydrophilic sequence. In helix-inducing solvent, dermaseptin *b* adopts an amphipathic α-helical conformation that most closely resembles class L amphipathic helixes, with all lysine residues on the polar face of the helix. The peptide exhibits growth inhibition activity *in vitro* against a broad spectrum of pathogenic microorganisms including yeast and bacteria as well as various filamentous fungi that are responsible for severe opportunistic infections accompanying acquired immunodeficiency syndrome and the use of immunosuppressive agents. Maximized pairwise sequence alignment of dermaseptin *b* and dermaseptin *s*, a 34-residue antimicrobial peptide previously isolated from *Phyllomedusa sauvagii*, reveals 81% amino acid identity. No other significant similarity was found between dermaseptin *b* and any prokaryotic or eukaryotic protein, but similarity was found with adenoregulin (38% amino acid positional identity), a 33-residue peptide that enhances binding of agonists to the A1 adenosine receptor. The synthetic replicates of dermaseptin *b* and adenoregulin displayed similar but nonidentical spectra of antimicrobial activity, and both peptides were devoid of lytic effect on mammalian cells. Accordingly, the observation that adenoregulin enhances binding of agonists to the adenosine receptor may in fact be a consequence of its ability to alter the structure of biological membranes and to produce signal transduction via interactions with the lipid bilayer, bypassing cell surface receptor interactions.

Protection of vertebrate animals against invading pathogens depends on a network of host-defense systems including highly specific cell-mediated immune responses. However, the growing number of reports of vertebrate peptides that exhibit broad-spectrum antimicrobial activity points to yet an unexpected additional strategy of circumventing host invasion and maintaining the growth of commensal microorganisms. This peptide-based defense system is separated from, but integrated with, the cell-mediated immune system and involves the synthesis of a battery of small-sized cationic peptides analogous to the insect cecropins (Boman & Hultmark, 1987) and defensins (Lambert *et al.*, 1989; Dimarcq *et al.*, 1992; Lehrer *et al.*, 1991). Antimicrobial peptides are produced by lymphoid tissues as well as by nonlymphoid cells of the skin, the respiratory tract, and the gastrointestinal system of vertebrates. The antibiotic effects of these peptides have been attributed to their lipid affinity and may be due to disruption of prokaryotic cell membranes followed by osmotic lysis (Giovannini *et al.*, 1987; Zasloff *et al.*, 1988). Mammalian defensins are examples of bactericidal sulfide bridged peptides, 29–34 residues in length, which are sequestered in granules of circulating neutrophils (Lehrer *et al.*, 1991) as well as in the Paneth cells of the small intestine (Ouellett *et al.*, 1989) and delivered to phagocytic vacuoles containing ingested microorganisms. In micromolar concentrations, these peptides causes cell lysis of a broad array of microorganisms *in vitro*, including Gram-positive and Gram-negative bacteria, yeast, and protoza (Stanfield *et al.*, 1988). Defensins are, however, cytolytic for eukaryotic cells including human cells.

Early attempts to detect antimicrobial substances from nonlymphoid cells have led to the discovery of a 24-residue cationic peptide, designated bombinin (Csordas & Michl, 1970), from the skin of the European toad *Bombina variegata*, although establishment of the complete amino acid sequence and activity spectrum of this class of peptides has only recently been achieved (Simmaco *et al.*, 1991; Gibson et al., 1991). Two highly similar 23-residue peptides, named magainins I and II (Zasloff, 1987) or, respectively, PGS and [Gly^{10},Lys^{22}]-PGS (Giovannini *et al.*, 1987; Terry *et al.*, 1988), have been isolated from the skin of the African clawed frog *Xenopus laevis*. The magainins, along with PGLa, PGK, CPF, and XPF (Bevins & Zasloff, 1990; Hoffmann *et al.*, 1983; Gibson *et al.*, 1986; Sures & Crippa, 1984), are all highly related basic (lysine-rich) peptides from the same source and display potent antimicrobial activity against Gram-positive and Gram-negative bacteria, as well as some yeast and protozoa (Soravia *et al.*, 1988). As such, these peptides seem to play an essential role in the defense of the skin of frogs against microbes and to aid in wound repair. It is worth pointing out that despite the activity of these peptides on prokaryotic membranes, they do not induce lysis of erythrocytes and other circulating cells of vertebrates (Zasloff, 1987; Chen *et al.*, 1988). This property may be related to the presence of cholesterol in eukaryotic cell membranes. While magainins and related antimicrobial peptides have little ordered structure in water, they reveal a potential for forming amphipathic α-helixes at hydrophobic–hydrophilic interfaces such as might occur at cell surfaces. This structure presumably underlies their lytic activity since several studies have indicated that the α-helical properties of these peptides, but not their primary sequence *per se*, are the most important features in the mechanism of action (Duclohier *et al.*, 1989; Matsuzaki *et al.*, 1989; Williams *et al.*, 1990; Cruciani *et al.*, 1991; Rana *et al.*, 1991; Chung *et al.*, 1992; Grant *et al.*, 1992).

Among the members of this small but growing family of vertebrate defensive peptides, a novel 34-residue peptide,

® Abstract published in *Advance ACS Abstracts,* April 15, 1994.

0006-2960/94/0433-6642$04.50/0

designated dermaseptin *s*, was recently isolated from the skin of the South American arboreal frog *Phyllomedusa sauvagii* (Mor *et al.*, 1991). Dermaseptin *s*, ALWKTMLKKLGTMALHAGKAALGAAADTISQGTQ, has little or no sequence homology with any other defensive peptides and is unique in that it is the first vertebrate peptide to show lethal effect against bacteria, yeast, and protozoa, as well as filamentous fungi responsible for severe opportunistic infections accompanying immunodeficiency syndrome and the use of immunosuppressive agents. However, dermaseptin *s* was shown to be inactive against mammalian cells (Mor *et al.*, 1991; Hernandez *et al.*, 1992). Theoretical predictions, model building, and circular dichroism studies indicated that dermaseptin *s* shares with the magainins a high propensity to fold in an amphipathic α-helical structure in α-helix-promoting solvents. Ultrastructural studies using electron microscopy and immunocytochemistry (Hernandez *et al.*, 1992) as well as electrophysiological studies using liposomal models (Pouny *et al.*, 1992) demonstrated that dermaseptin *s* kills microorganisms through selective lysis of biological membranes.

A peculiar property of amphibians is the marked ability of subspecies to produce their own set of antimicrobial peptides that often differ with but a few amino acid substitutions. In that regard, we expected *Phyllomedusa bicolor* skin to contain other dermaseptin-like peptides with distinct spectra of antifungal activity, as unlike antibacterial products, the therapeutic armamentarium against fungal infections is rather scarce. Toward this goal, and to investigate the modes of production of these peptides, several live specimens of *P. bicolor* were captured in Guyana and brought to the laboratory, where they have been bred. In this study, we report the isolation, structural characterization, and activity of a novel peptide that exhibited potent antimicrobial activity against a large spectrum of pathogenic microorganisms. The relationship between this peptide and adenoregulin is highlighted.

MATERIALS AND METHODS

Purification of Dermaseptin b from Frog Skin Extract. The skin and adherent tissues from one specimen of *P. bicolor* were minced with scissors and extracted three times for 1 h each in 20 volumes (v/w) of 10% acetic acid at room temperature. Combined extracts were centrifuged for 30 min at 3000*g*, and the supernatant was lyophilized. The dried extract was dissolved in 10% acetic acid and fractionated on a calibrated gel filtration column (Sephadex G-50 superfine, 1.5 × 100 cm). Fractions (4 mL) were collected at a flow rate of 10 mL/h, from which combined aliquots (100 μL) from each three fractions were pooled, lyophilized, and assayed for antifungal activity as described below. Active fractions (fractions 80–90) were pooled and evaporated under vacuum (yield = 125 mg). This material was subjected to reversed-phase HPLC chromatography on a preparative C_{18} column (RCM 10 × 25) loaded with 60 mg of extract in 0.75 mL of water containing 0.1% trifluoroacetic acid. After an initial 5-min wash in 0.1% trifluoroacetic acid/water, elution was achieved at a flow rate of 7 mL/min with a 0–60% linear gradient of acetonitrile containing 0.07% trifluoroacetic acid (from 5 to 65 min); 3.5-mL fractions were collected from which an aliquot (100 μL) was assayed for antifungal activity. Fractions that eluted at 71–72 min were further fractionated on a Nucleosil C_4 analytical HPLC column (300 Å, 5 μm, 250 × 4.6 mm) using a 20–60% (0.5%/min) linear gradient of acetonitrile containing 0.1% trifluoroacetic acid and 0.2% triethylamine at a flow rate of 0.5 mL/min. The final purification step was performed on an analytical Delta-Pac HPLC column (Waters, C_{18}, 5 μm, 150 × 2 mm) eluted at a flow rate of 0.2 mL/min with 35% acetonitrile in 0.1% trifluoroacetic acid/water.

Solid-Phase Peptide Synthesis. Dermaseptin *b*, dermaseptin *s*, and adenoregulin were prepared by stepwise solid-phase synthesis using fluoren-9-ylmethoxycarbonyl (Fmoc) polyamide active ester chemistry on a Milligen 9050 pepsynthesizer. All Fmoc-amino acids were from Milligen. HMP-linked polyamide/kieselguhr resin (pepsin KA), Fmoc-amino acid pentafluorophenyl (Pfp), and 3-hydroxy-2,3-dehydro-4-oxobenzotriazine (Dhbt) esters were from Milligen. Side-chain protection for Asp and Thr was *t*-Bu and for Lys and His Boc. Cleavage of peptidyl resin and side-chain deprotection were carried out at a concentration of 10 mg of peptidyl resin in 1 mL of trifluoroacetic acid/phenol (95%/5% v/v) for 2 h at room temperature. After filtration to remove the resin and ether extraction, the crude peptides were purified by a combination of Sephadex gel filtration, ion-exchange chromatography, and preparative HPLC. Homogeneity of the synthetic peptides was assessed by analytical HPLC, amino acid analysis, solid-phase sequence analysis, and mass spectrometry as described (Nicolas *et al.*, 1986).

Amino Acid Analysis and Amino Acid Sequence Analysis. The amino acid composition was determined on an hydrolysate of the peptides (250 pmol) after phenylthiocarbamylation of the released residues by phenyl isothiocyanate followed by HPLC analysis as previously described (Nicolas *et al.*, 1986). Sequence analysis was carried out on a Milligan 6600 solid-phase sequencer after covalent binding of the samples to Sequelon arylamine membranes. Phenylthiohydantoin amino acids were detected with an on-line HPLC column (Waters MS HPLC; Sequa Tag C_{18} PTH analysis column, 350 × 3.9 mm) developed with ammonium acetate (pH 4.8) and acetonitrile and calibrated with 15 pmol of phenylthiohydantoin amino acid standards. Data collection and analysis were performed with a Maxima-PTH chromatography analysis software package (Dynamic Solution Corp., Division of Waters Chromatography, Milford MA).

Electrospray Ionization Mass Spectrometry. Mass spectral analysis was performed using a quadrupole coupled electrospray mass spectrometer (Nermag R10-10) associated with a source produced by Analytica of Branford. The mass scale was calibrated using three peptides whose protonated masses were 574.22, 768.30, and 1046.54, respectively; the accuracy was estimated to be ±0.5 Da. Samples were dissolved in a water/methanol (1:1) mixture and introduced via a metal capillary (stainless steel) at atmospheric pressure at a rate of 1 μL/min using a microliter syringe installed in a syringe infusion pump (Harvard Apparatus Model 11). An electrospray voltage of −5 kV was applied to the internal wall of the source at the origin of the liquid dispersion for an electrospray formation and ion extraction. Ions were detected and analyzed in the positive mode as a function of their m/z ratio.

Circular Dichroism Measurement. Peptide samples were dissolved in water (0.05 mg/mL) or in 20% trifluoroethanol/water (v/v). Spectra were obtained in a Jobin-Yvon Mark IV instrument linked to a Minc digital II miniprocessor, at room temperature using a quartz cuvette of 1 mm path length. CD data represent average values from six separate recordings. The contents of α-helix, β-sheet, and unordered structures were estimated as described (Yang *et al.*, 1986).

Antimicrobial and Hemolytic Assays. Antifungal activity of extracted material was evaluated as follows: 5 mL of Sabouraud glucose broth (SM) containing 20 g/L agar was poured over a Petri dish. After solidification, the plate was

inoculated with microconidia of *Aspergillus fumigatus* (IP864) and incubated for 48 h at 27 °C, and then the culture was submerged in SM for 1 h. Thin slices (3 × 3 mm) of gel containing the growing part of the mycelium were cut, transferred onto a microdish, incubated in SM in the presence of an aliquot from chromatography fractions, freeze-dried, and solubilized in 15 μL of SM. Minimal inhibitory concentrations for DS *b*, DS *s*, and adenoregulin were determined using the synthetic replicates after purification to homogeneity. The purified peptides were weighed in a microbalance and solubilized in water at the desired primary dilution. Each peptide solution was assayed with the various strains in sterilized 96-well plates (Nunc F96 microtiter plates, Denmark) in a final volume of 100 μL composed of 50 μL of suspension containing 1 × 10^6 spores or microcodia/mL in Sabouraud glucose broth or 1 × 10^6 bacteria/mL in Luria Bertani (LB) culture medium and 50 μL of synthetic peptide in serial 2-fold dilutions in water. Each MIC was determined from two independent experiments performed in duplicate. Positive and negative controls were, respectively, water and 0.1% formol/water added to the same suspension. Inhibition of growth was determined by measuring optical density at 492 nm with a Titertek Multiskan MCC after an incubation time of 48 h at 30 °C (37 °C for bacteria).

Hemolytic activity of DS *b*, DS *s*, and adenoregulin was assayed with fresh human or rabbit blood, drawn directly onto a syringe containing EDTA (50 mM) and rinsed three times in PBS (50 mM sodium phosphate, 150 mM NaCl, pH 7) by centrifugation for 15 min at 1600 rpm (*g* × 490). Red blood cells (62.5 μL, 1 × 10^8/mL) in PBS were then incubated at 37 °C with 62.5 μL of distilled water (positive control), with 62.5 μL of PBS (negative control), or with 62.5 μL of increasing concentrations of synthetic DS *b* in PBS. Release of hemoglobin was monitored after centrifugation by measuring the optical density of 100 μL of supernatant at 541 nm.

RESULTS

Isolation and Purification of Dermaseptin b. Dermaseptin *b* (DS *b*) was purified to homogeneity from *P. bicolor* skin extract by a two-step protocol involving size fractionation and reversed phase high-performance liquid chromatography. Antifungal activity was used as a functional assay. The absorbance profile, at a wavelength of 280 nm, of a gel filtration fractionation on a calibrated Sephadex G-50 column is shown in Figure 1A along with the antifungal activity profile. Fractions 80–90 containing the peak antifungal activity were pooled (yield = 125 mg) and further fractionated by reversed-phase HPLC preparative column. As shown in Figure 1B, the initial antifungal activity from G-50 was recovered as three distinct active peaks eluting at 41, 64, and 71 min, respectively. The latest eluting peak was further purified using a series of analytical HPLC runs operating with successively slower gradients of acetonitrile. At this point, a well-separated UV-absorbing peak was obtained (inset, Figure 1B) which contained a homogeneous peptide (yield = 15 μg/g of original wet tissue) exhibiting fungal growth inhibition against *A. fumigatus* at concentrations estimated to be in the micromolar range (Figure 2) and 100% lysis at 60 μM as determined by MIC experiments (Table 2). The purified peptide (95% purity as determined by microbore HPLC) was directly subjected to amino acid analysis and protein sequence analysis.

Amino Acid Sequence Analysis and Mass Spectral Analysis. The amino acid composition of the purified antifungal peptide determined after acid hydrolysis was Asx (1.9), Glx (1.3), Ser (1.1), Thr (2.2), Gly (3.0), His (0.9), Ala (5.8), Val

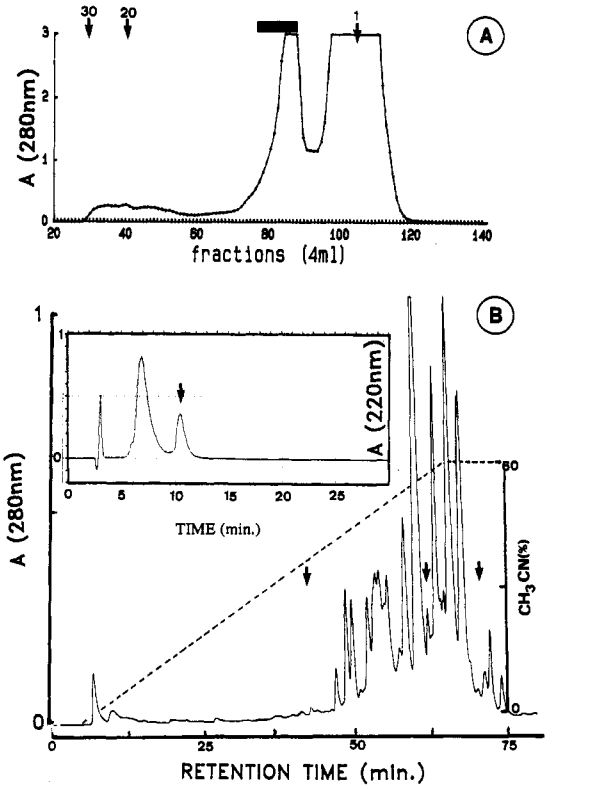

FIGURE 1: Purification of dermaseptin *b* from *P. bicolor* skin. (A) Size fractionation profile of the skin extract on a Sephadex G-50 (superfine) column (2.4 × 100 cm) using 10% acetic acid as eluant. Four-milliliter fractions were collected at a flow rate of 10 mL/h. Arrows point to the elution positions of molecular weight markers (× 10^{-3}). The *bar* indicates antifungal activity and the *solid line*, absorbance at 280 nm. (B) Reversed-phase HPLC chromatogram of fractions 80–90 from the G-50 column. Fractions were pooled (yield = 60 mg), concentrated under reduced pressure, and loaded onto a preparative C_{18} HPLC column (RCM 10 × 25 mm) equilibrated with 0.1% trifluoroacetic acid in water. Elution was achieved at a flow rate of 7 mL/min with a linear gradient of acetonitrile containing 0.07% trifluoroacetic acid. *Arrows* point to positions of antifungal fractions. The *solid line* indicates absorbance at 280 nm and the *dashed line*, percent acetonitrile. (Inset) Final reversed-phase HPLC purification step of DS *b*. Fraction 71 from (B) was recovered and loaded onto an analytical Delta-Pac (Waters, C_{18} 5 μm, 150 mm × 2 mm) HPLC column. Elution was achieved under isocratic conditions with 35% acetonitrile in 0.1% trifluoroacetic acid/water. Fractions (0.2 mL) were collected at a flow rate of 200 μL/min. The *arrow* points to the elution position of synthetic DS *b*. The *solid line* indicates absorbance at 220 nm and the *dashed line*, percent acetonitrile.

(3.2) Leu (3.0, Ile 1.9, and Lys (2.9). The peptide was calculated to contain 27 amino acid residues with no estimation of tryptophan. In fact, inspection of the near-UV spectra of the peptide indicated the absence of the classical tryptophan UV signature. As expected from reversed phase HPLC, the antifungal peptide is rich in hydrophobic residues. However, the sequence of the peptide was determined only up to the 23rd residue as DVLKKIGTVALHAGKAALGAVAD by automated Edman degradation on a solid-phase sequencer after carboxylic covalent binding of the sample (150 pmol) to Sequelon arylamine membrane (Figure 3).

Comparison of the amino acid composition and amino acid sequence revealed the peptide to contain an additional tetrapeptide (Thr, Ile, Ser, Glx). These results suggested that the complete peptide sequence was not obtained due to the occurrence of a carboxamidated COOH terminus and permitted the assignment of Glx as glutamine. In that case, Edman degradation of the carboxylic-linked peptide would indeed allow the determination of the sequence only up to

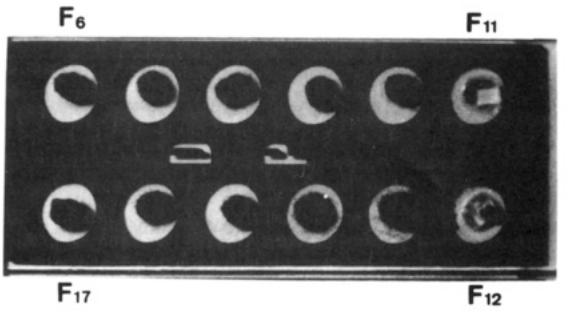

FIGURE 2: Antifungal activity of analytical reversed-phase HPLC fractions. Assay of growth inhibition was performed with a 48-h-old *A. fumigatus* cultured on agar gel. Each slice was exposed to a 20-μL aliquot of HPLC fractions corresponding to those in the inset of Figure 1B. Microdishes were incubated at 30 °C for 24 h in Sabouraud glucose broth. Clear areas indicate growth inhibition of *Aspergillus*. In the experiment shown, inhibitory activity is observed for HPLC fractions 11 and 12.

Asp[23] anchored through its side chain, whereas the C-terminal fragment, residues 24–27 being devoid of free acidic group, would be undetectable. Additional confirmation was obtained by mass spectral analysis of the peptide using electrospray ionization mass spectrometry. As shown in Figure 3C, three unequivocal pseudomolecular ions $[M + nH]^{n+}$ were observed at m/z values corresponding to $n = 2$, 3, and 4 protonated species. A fourth molecular ion was observed at m/z 1766.93 that corresponds to a dimer. The molecular weights calculated for the most intense peaks were 2646.14 ($n = 2$), 2646.81 ($n = 3$), and 2646.72 ($n = 4$). These values confirmed the amino acid composition of the peptide as they corresponded to that expected theoretically for the experimentally determined amino acid sequence (2647.14), with a carboxamidated C-terminal extension (Ser, Thr, Ile, Gln) and no other additional posttranslational modifications.

Table 1: Maximized Pairwise and Multiple Sequence Alignments of Dermaseptin *b* (DS *b*), Dermaseptin *s* (DS *s*), and Adenoregulin (ADR)[a]

Peptide	Amino acid sequence	Similarity score
DS b	....DVLKKIGTVALHAGKAALGAVADTISQ...	
DS s	ALWKTMLKKLGTMALHAGKAALGAAADTISQGTQ	
	-***-**-********** ******	81.4 %
DS b	DVLKKIGTVALH.....AGKAALGAVADTISQ	
ADR	GLWSKIKEVGKEAAKAAAKAAGKAALGAVSEAV..	
	-- ** *- - ********----	38.4%
DS b	....DVLKKIG.....TVALHAGKAALGAVADTISQ...	
DS s	ALWKTMLKKLG.....TMALHAGKAALGAAADTISQGTQ	
ADR	GLWSK.IKEVGKEAAKAAAKAAGKAALGAVSEAV.....	
	-* -* - * ******** ----	34 %

[a] Pairwise and multiple sequence alignments were performed by using CLUSTAL V Multiple Sequence Alignment software (Higgins & Sharp, 1989) with fixed gap penalty. A Dayhoff PAM 250 matrix is used in peptide comparisons (Dayhoff et al., 1978). The similarity scores for pairwise sequence alignments are calculated according to the method of Wilbur and Lipman (1983). Identical (*) and similar (–) residues among sequences are highlighted. Gaps (.) have been introduced to maximize sequence similarities.

The search for similarity between the partial amino acid sequence of the novel antifungal peptide and the sequence of dermaseptin *s* (Mor *et al.*, 1991), a 34-residue antimicrobial peptide previously isolated from the skin of *P. sauvagii*, was carried out using CLUSTAL V Multiple Sequence Alignment software (Higgins & Sharp, 1989). As shown in Table 1,

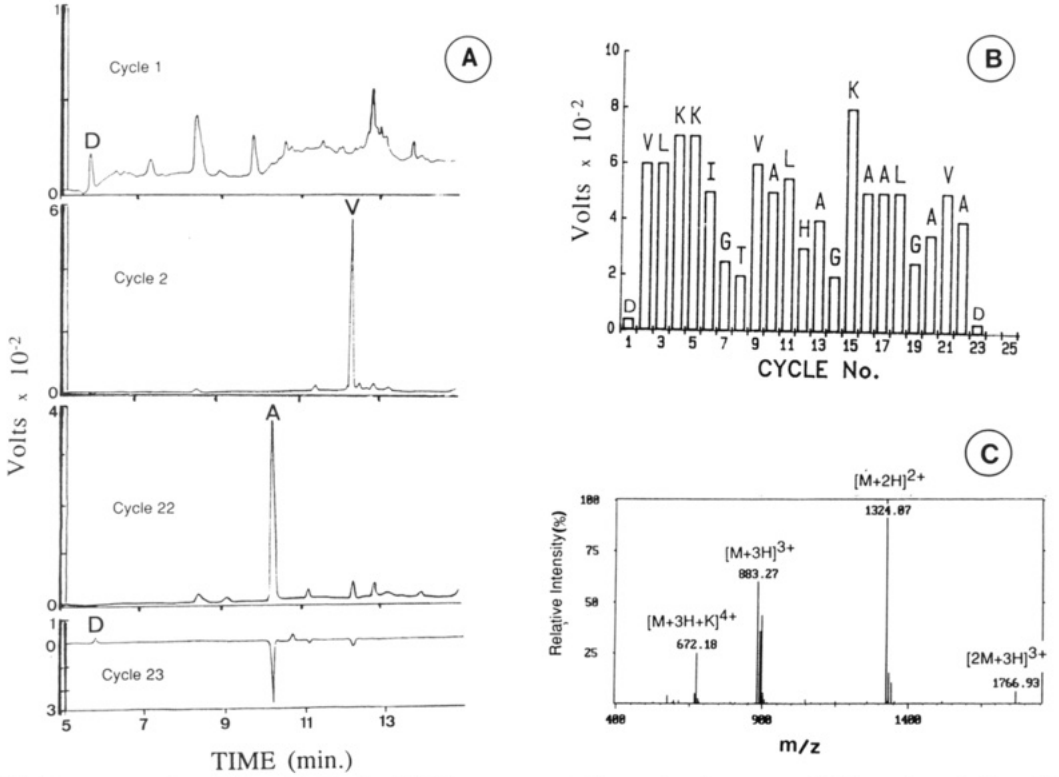

FIGURE 3: Solid-phase sequencing of dermaseptin *b*. (A) Four representative cycles of automated Edman degradation. The three upper diagrams are the raw HPLC absorbance profiles obtained at cycles 1, 2, and 22, respectively. The fourth diagram represents the differential profile obtained from the subtraction of cycle 23 from cycle 22 using dynamic alignment of data sets. The *solid line* indicates absorbance at 269 nm (313 nm for Ser and Thr). Amino acid PTH identification is shown using the single-letter code. (B) Repetitive PTH intensities obtained from overall cycles. (C) Electrospray ionization mass spectrum of DS *b* showing three multiple ions whose average mass is 2647.1. The peak at m/z 1766.93 is a dermaseptin *b* dimer.

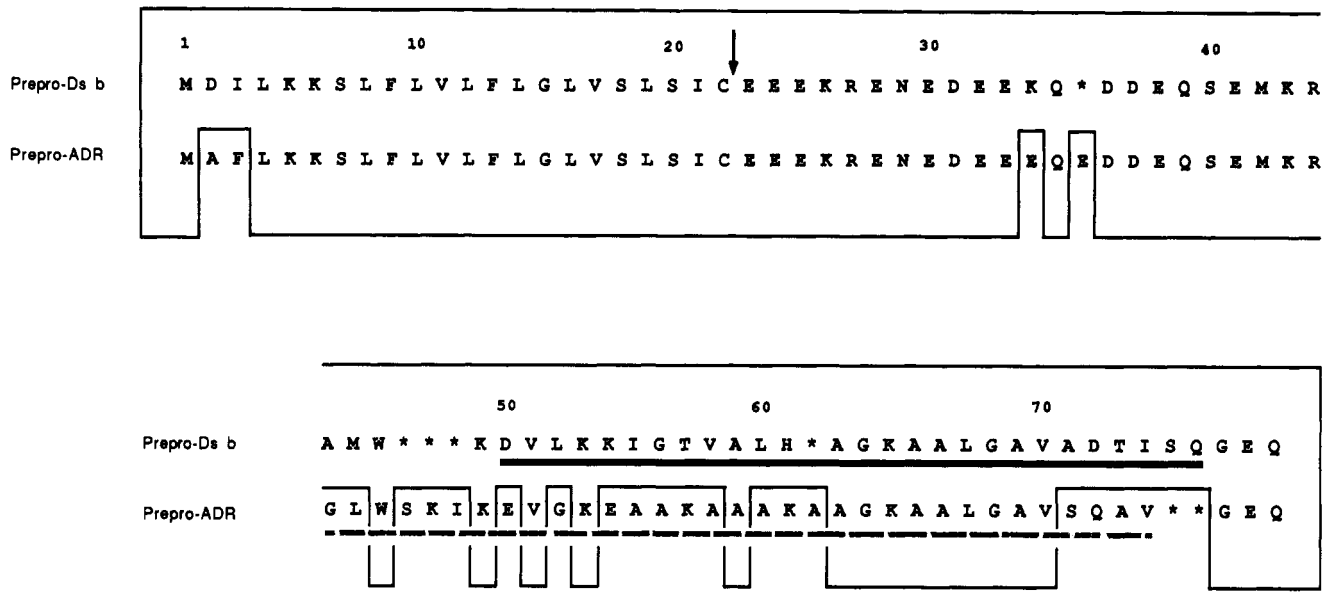

FIGURE 4: Amino acid sequence of preprodermaseptin *b* and preproadenoregulin. Regions of identity between the two precursor sequences are boxed. Gaps (asterisks) have been introduced to maximize similarity. The arrow indicates the common carboxy-terminal cleavage site for the signal peptides. The numbering refers only to preprodermaseptin *b*. A solid line is drawn under the amino acid sequence of dermaseptin *b*. A dashed line is drawn under the amino acid sequence of adenoregulin.

pairwise alignment of the two sequences revealed 78% amino acid positional identity. In particular, the sequence of the novel antifungal peptide closely resembles that of the central core, residues 7–27, of dermaseptin *s*: ALWKTM LKKLGTMALHAGKAALGAAADTISQGTQ. On the basis of the high level of sequence similarity with dermaseptin *s*, we proposed the primary structure of the novel 27-residue peptide to be DVLKKIGTVALHAGKAALGAVADTISQ-NH_2. Accordingly, the novel peptide was designated dermaseptin *b*.

A definitive confirmation of the structure proposed for dermaseptin *b* was obtained recently through molecular cloning of the dermaseptin *b* biosynthetic precursor from *P. bicolor* skin. As shown in Figure 4, the dermaseptin *b* precursor protein deduced from the cDNA sequence is 78 residues long (Amiche *et al.*, submitted for publication) and contains a putative signal sequence at the N terminus, a 20-residue spacer sequence extremely rich in acidic amino acids, a pair of basic residues (Lys^{43}-Arg^{44}), and a single copy of a dermaseptin *b* progenitor sequence at the COOH terminus followed by an extra tripeptide (GEQ). Since the C terminus of native dermaseptin *b* is blocked by an amide group, it is expected that removal of the dipeptide EQ by a carboxypeptidase or by a dipeptidyl carboxypeptidase would expose the extra glycine adjacent to Gln^{75} at the C terminus of the dermaseptin *b* progenitor sequence, and this could be converted into a desglycine peptide amide by a two-step amidating reaction (Bradbury & Smyth, 1991). Although there is complete agreement between the proposed amino acid sequence of dermaseptin *b* and that of residue 49–75 of preprodermaseptin *b* as predicted from the cDNA, there is coding information in the clone for an additional tetrapeptide (AMWK) at the amino end of dermaseptin *b*. Since this structure is missing from dermaseptin *b* as isolated from frog skin, it may have been removed by the proteolysis *in vivo*.

Solid-Phase Synthesis of Dermaseptin b. To confirm that antimicrobial activity of native dermaseptin *b* reflected intrinsic properties, the peptide was synthesized by the solid-phase method. Purification of the synthetic peptide was by gel filtration, ion-exchange chromatography, and reversed-phase HPLC. After purification, synthetic dermaseptin *b* was shown to be indistinguishable from natural dermaseptin *b* by the following chemical and physical criteria. The purified synthetic peptide showed by HPLC a unique sharp peak eluting at the position of the corresponding natural product (Figure 1), and co-injection of the two peptides resulted in only one peptide peak (data not shown). The sequence of synthetic dermaseptin *b* could be determined only up to Asp^{23} by automated Edman degradation after covalent binding of the peptide to Sequelon arylamine membrane. Mass spectrometry of a sample of synthetic dermaseptin *b* gave pseudomolecular ions $(M + nH]^{n+}$ at m/z values corresponding to $n = 2, 3$, and 4 protonated species, exactly as obtained from the natural peptide. Final confirmation of the structural identity between natural and synthetic dermaseptin *b* was achieved by submitting the synthetic peptide to digestion with trypsin. The digest was analyzed by HPLC and proved to be identical to that generated from natural product (data not shown). Since the synthetic product was found to be indistinguishable from its natural counterpart, it was used in the following to evaluate its antimicrobial spectrum and its conformation.

Antimicrobial Activity of Dermaseptin b. Dermaseptin *b* was investigated for its ability to affect the vital prognostic of various prokaryotic and eukaryotic cells in culture media. Its ability to inhibit cell proliferation is reported in terms of minimal inhibitory concentration (MIC), defined as the dose at which 100% inhibition of growth was observed after 48 h of incubation at 30 °C (37 °C for bacteria). In the presence of micromolar concentrations, dermaseptin *b* inhibited by 100% the proliferation of most microorganisms tested, including Gram-positive or Gram-negative bacteria, yeast, and pathogenic filamentous fungi (Table 2). Interestingly, the dose–response profiles obtained showed sharp curves in which 0–100% inhibition was generally observed within a 2-fold peptide dilution (data not shown). However, dermaseptin *b* exhibited significantly lower potencies than dermaseptin *s*, namely against the yeasts *Cryptococcus neoformans* and *Candida albicans*, or against the bacteria *Aeromonas caviae*, *Pseudomonas aeroginosa*, *Enterococcus faecalis*, *Escherichia coli*, and *Staphylococcus aureus*. The cytotoxicity of dermaseptin *b* toward mammalian cells was assessed against human and rabbit erythrocytes. After a 1-h treatment,

Table 2: Antimicrobial Spectra of Dermaseptin *b* (DS *b*), Dermaseptin *s* (DS *s*), and Adenoregulin (ADR)

organism	MIC[a] (μM) DS *b*	DS *s*	ADR
Cryptococcus neoformans (IP960-67)	60	5	5
Cryptococcus neoformans (IP962-67)	60	5	nd[b]
Candida albicans (IP884-65)	60	20	5
Candida albicans (IP886-65)	60	20	nd
Microsporum canis (IP1194)	20	15	3
Tricophyton rubrum (IP1400-82)	40	35	5
Tricophyton rubrum (IP2043-92)	40	35	nd
Tricophyton mentagrophytes (IP877-71)	40	30	nd
Arthroderma simii (IP1063-74)	40	30	10
Arthroderma simii (IP903-65)	40	30	nd
Aspergillus fumigatus (IP1025-70)	60	30	20
Aspergillus niger (IP218-53)	40	30	nd
Aeromonas caviae (IP67-16T)	60	5	20
Pseudomonas aeroginusa (IP76110)	>75[c]	30	nd
Escherichia coli (IP76-24)	50	2	5
Enterococcus faecalis (IP103214)	60	5	nd
Staphylococcus aureus (IP76-25)	>75	10	nd
Nocardia brasiliensis (IP16-80)	60	60	10

cell	hemolytic activity[d] (μM) DS *b*	DS *s*	ADR
human erythrocytes	>300[e]	>75	>75
rabbit erythrocytes	>300	>75	>75

[a] The minimal inhibitory concentration is defined as the dose at which 100% inhibition of growth was observed after 48 h of incubation in culture media. These concentrations represent mean values (±30%) of two independent experiments performed in duplicate. [b] Not determined. [c] No inhibitory effect was observed up to 75 μM. [d] Hemolytic activity after 1 h of incubation. [e] No toxic effect was observed up to 300 μM.

dermaseptin *b* did not permeate erythrocytes up to the highest concentration tested (1000 μg/mL).

Dermaseptin b Is Configured as a Class L Amphiphatic α-Helix. Prediction of the secondary structure of dermaseptin *b* according to the Information Theory (Garnier *et al.*, 1978) identified no less than 85% helical zone and 15% coil. Tentative localization of the helix indicated a domain spanning residues 1–23. When plotted as an α-helical wheel (Schiffer & Edmunson, 1967), hydrophobic and hydrophilic domains are clearly distinguishable (Figure 5). In this conformation, there are 8 hydrophilic or charged residues on one side of the cylindrical surface and 15 hydrophobic residues with no charged residue on the opposite side. The polar face of dermaseptin *b* subtends an average angle of 115° perpendicular to the long axis of the helix. Interestingly, the three lysine residues are not clustered toward the center of the polar face, as is often observed for other class L amphipathic helices (Segrest *et al.*, 1990), but are distributed around the perimeter of the polar side. The value of the mean angle subtended by positively charged residues is 115°. The only residues that appear not to fit the regular pattern of amphiphilicity are those of the C-terminal end, i.e., residues 25–27. This suggests that dermaseptin *b* can be configured as an amphipathic α-helix spanning residues 1–23.

Support for this proposal was obtained through CD measurements of dermaseptin *b* either in water or in a helix-promoting solvent. The far-UV CD spectra of dermaseptin *b* in water (Figure 6) was characteristic of nonstructured conformation. In the presence of a low concentration of trifluoroethanol, however, dermaseptin *b* became structured with a high level, i.e., 70%, of α-helix conformation (Yang *et al.*, 1986). No concentration dependency was observed in the range 10–200 μM. Hence, both theoretical predictions and CD measurements suggest that dermaseptin residues 1–23 can form a nearly perfect amphipathic α-helix in a low-polarity medium.

DISCUSSION

A novel antimicrobial peptide, designated dermaseptin *b*, has been purified to homogeneity from frog skin. Dermaseptin *b* is 27 amino acids long, containing 3 lysine residues that punctuate an alternating hydrophilic and hydrophobic sequence. Dermaseptin *b* differs from dermaseptin *s*, a 34-residue cationic antimicrobial peptide recently isolated from *P. sauvagii* skin, by several substitutions and deletions. However, pairwise alignments of the amino acid sequences of dermaseptin *b* and dermaseptin *s* yielded a similarity score of 81% (Table 1). This property, along with their antimicrobial activity, suggests that the two peptides are homologous and are products of genes that are members of the same family.

No other significant similarity was found between dermaseptin *b* and any prokaryotic or eukaryotic peptide or protein except with adenoregulin, a 33-residue cationic peptide recently isolated from *P. bicolor* skin (Daly *et al.*, 1992). For instance, pairwise sequence alignment of dermaseptin *b* and adenoregulin revealed 38% amino acid positional identity (Table 1). Similarly, dermaseptin *s* and adenoregulin exhibit 62% similarity score. In addition, synthetic adenoregulin exhibits antimicrobial activity against bacteria as well as yeast and fungi with potencies that are similar to, or higher than, those of the dermaseptins (Table 2). Yet, the three peptides do not permeate erythrocytes. These findings suggest that adenoregulin should be considered as a member of the dermaseptin family of antimicrobial peptides. Support for this proposal was obtained through cloning of the respective biosynthetic precursors of dermaseptin *b* and adenoregulin (Amiche *et al.*, submitted for publication). As shown in Figure 4, prepro-dermaseptin *b* and preproadenoregulin are very similar: 91% amino acid identity between the signal peptides and 82% identity between the acidic spacer sequences. In both precursors, the bioactive progenitor sequence is flanked by a pair of basic residues, Lys-Arg, at its amino end and a tripeptide, Gly-Glu-Gln, at its C terminus. This similarity also extends into the 5′-untranslated (70% nucleotide positional identity) and 3′-untranslated (75% nucleotide positional identity) regions of the mRNAs (not shown). The above findings suggest that the dermaseptins and adenoregulin are products of a single family of genes which are involved in the synthesis of small, lysine-rich, lytic peptides to provide frogs with a chemical defense system against microbial infections. Hence, the interesting observation that adenoregulin enhances binding of agonists to the A1 adenosine receptor activity (Daly *et al.*, 1992) may in fact be a consequence of the peptide ability to produce signal transduction via interaction with the lipid bilayer, bypassing cell surface adenosine–receptor interaction.

The propensity of small-sized cationic peptides to form α-helical amphipathic structure in apolar medium has been proposed as a prerequisite for their membrane lytic activity. However, this pattern is a very general attribute that is common to a variety of peptides and proteins that do not disrupt biological membranes. A detailed analysis of the physicochemical and structural properties of amphipathic α-helixes in several peptides and proteins has led Segrest and co-workers to distinguish seven classes of amphipathic helixes (Segrest *et al.*, 1990). According to this classification, lytic peptides belong to the class L of α-helixes which have a highly positively charged and narrow polar face, a mean lysyl/arginyl ratio of 30, and a highly hydrophobic apolar face. Secondary structure

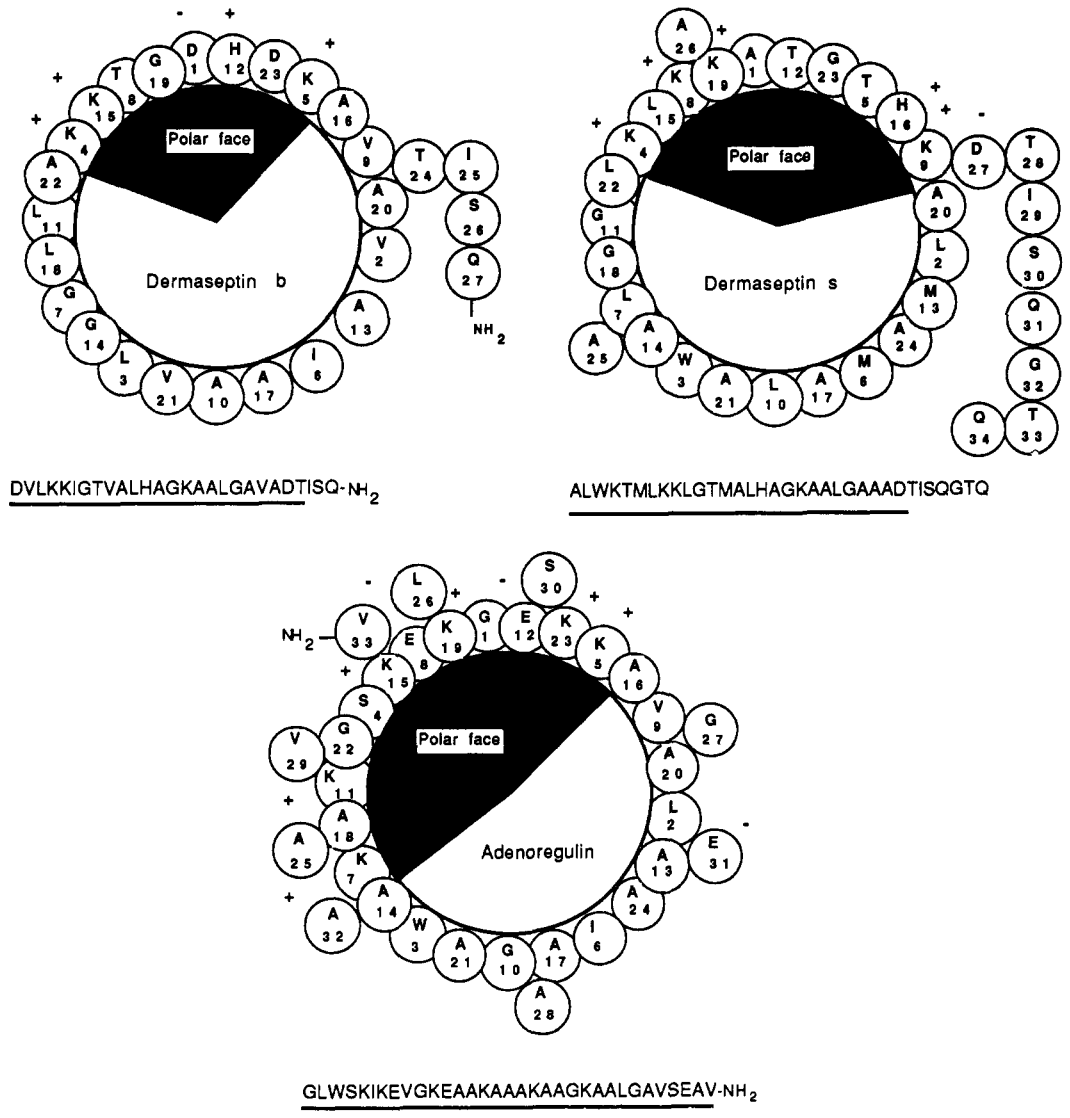

FIGURE 5: α-Helical wheel plots of dermaseptin *b*, dermaseptin *s*, and adenoregulin showing their amphipathic structure. In this conformation, periodic variation in the hydrophobicity value of the residues along the peptide backbone with a 3.6 residues/cycle period characterizes an α-helix (Schiffer & Edmunson, 1967). A charged hydrophilic domain (black) and a hydrophobic domain (white) are clearly distinguishable on the cylindrical surface of each peptide. The amino acid sequence of the peptides is shown underneath the corresponding wheel plot. Helical domains as predicted by the Information theory (Garnier *et al.*, 1978) are underlined.

prediction of dermaseptin *s* and dermaseptin *b* based on the Information theory (Garnier *et al*, 1978) and circular dichroism studies showed 75% and 85% α-helical contents, respectively. Each peptide can be fitted to a well-behaved class L amphipathic helix (Figure 5) with hydrophobic residues on one face of the structure and polar or charged residues on the opposite face. Theoretical prediction also showed that adenoregulin can form a cationic amphipathic α-helix in which the charged residues are clustered on one face of the cylindrical surface (Figure 5). In all three helixes, the lysine residues are not clustered toward the center of the polar faces (Segrest *et al.*, 1990) but randomly distributed around the perimeter of the polar faces. Although dermaseptin *b* and dermaseptin *s*, as well as adenoregulin, belong to the class L of amphipathic helixes, their polar faces exhibit significant differences from one another. For instance, dermaseptin *b* has a narrow polar face subtending a mean radial angle of 115°, a value close to the average value (100°) for class L amphipathic helixes (Segrest *et al.*, 1990). In contrast, the polar face of dermaseptin *s* is wider, averaging 145°, whereas that of adenoregulin covers half of the cylindrical surface, being 175° in width. Moreover, there is a great variation in the charge density and net charge of the polar face of the peptides. There are six lysines and two glutamic acids on the polar face of adenoregulin, while only three lysines and one or two aspartic acids are found on that of dermaseptins *s* and *b*, respectively. These differences may account for the differences observed in their spectra of activity. In this regard, the physiological significance of the occurrence of whole families of antimicrobial peptides as the dermaseptins in *Phyllomedusa*, the bombinins in *Bombina*, and the magainins in *Xenopus* may be to provide a broader spectrum of activity against invading microorganisms. For instance, dermaseptin *s* and adenoregulin are highly active against several Gram-positive and Gram-negative bacteria as well as various yeast strains and fungi (Table 2). Although both peptides share a similar antimicrobial spectrum, there are substantial differences in their potency to kill microorganisms. Whereas adenoregulin showed a potent inhibitory activity against *Cryptococcus* and *Aspergillus* with minimal inhibitory concentrations that are similar to those of dermaseptin *s*, it killed *Candida*, *Microsporum*, *Tricophyton*, *Arthroderma*, and *Nocardia* with 3–7-fold higher potencies than dermaseptin *s*. On the other hand, adenoregulin is 3–4-fold less efficient than dermaseptin *s* in killing *Aeromonas* or *Escherichia*. A similar conclusion can be drawn when antimicrobial potencies of dermaseptin *b*

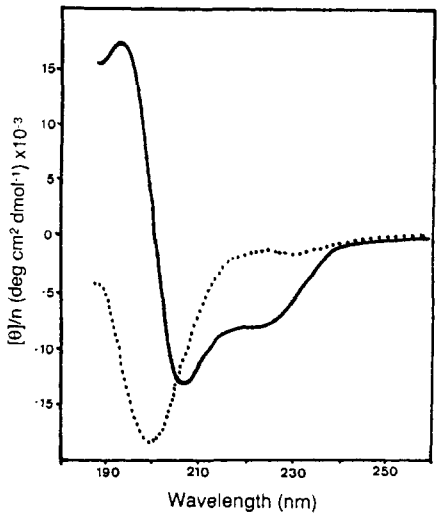

FIGURE 6: Far-UV circular dichroism spectra of synthetic dermaseptin *b* in water (0.05 mg/mL), in the absence (*dotted line*) or the presence (*solid line*) of trifluoroethanol. The spectrum in pure water is characteristic of an unordered structure. In the presence of 20% trifluoroethanol, the peptide becomes structure, exhibiting a high level of helical folding.

and dermaseptin *s* (Table 2) are compared. These differences may be relevant to some of the differences between the structure and the amino acid composition of the polar faces of the three peptides. In particular, the presence of six lysine residues on the polar face of adenoregulin versus three in the dermaseptins may allow deeper destabilization of membrane integrity by the former peptide and hence higher antimicrobial potency.

Despite the overall structural and pharmacological analogy between dermaseptins *b* and *s*, these peptides differ with respect to their biosynthesis and posttranslational maturation. Besides some point substitutions involving analogous hydrophobic amino acids, e.g., Leu/Ile or Met/Val, dermaseptin *b* presents a central region that is highly similar to that of dermaseptin *s*, with marked differences at both termini. In addition, the C-terminal end of dermaseptin *b* is shorter and carboxyamidated. The N terminus of dermaseptin *b* is also shorter than that of dermaseptin *s* and clearly less hydrophobic. Interestingly, the N-terminal tetrapeptide ALWK is present in the coding part of preprodermaseptin *b* (Figure 4). Overall, these differences may account for the fact that dermaseptin *b* presented qualitatively similar but less potent antimicrobial activity than the *P. sauvagii* peptide, dermaseptin *s* or its analog DS-[1–18]-NH_2, exhibiting lower MICs under the same set of conditions (Mor & Nicolas, 1994).

Although the mechanism of action of the dermaseptins remains to be clearly established, it is probable that their antimicrobial activity is due to surface-active properties that lead to disturbance of membrane functions (Hernandez *et al.*, 1992; Pouny *et al.*, 1992; Mor & Nicolas, 1994) as suggested for other cationic amphipathic peptides such as magainins, PGLa, PGK, CPF, and XPF (Hoffman *et al.*, 1983; Sures & Crippa 1984; Gibson *et al.*, 1986; Soravia *et al.*, 1988). All of these peptides are small-sized (21–34 residues), polycationic, and potentially amphipathic. These features characterize all of the hitherto known antimicrobial peptides synthesized by frog skin and suggest that they act via similar mechanisms to permeable microbial membranes despite the remarkable differences in their primary structure. Whereas most antimicrobial peptides also show potent activity mainly against bacteria, peptides of the dermaseptin family are among the rare and interesting examples of vertebrate molecules that develop a large spectrum of antibiotic activity, including against pathogenic fungi, as, unlike antibacterial products, there are only a few efficient agents developed in the therapy of fungal infections. Since dermaseptins have no sequence identity with the known amphibian peptide antibiotics, they should be a useful tool for identifying key features and conformational determinants responsible for membrane permeabilization.

Amphibian skin extracts contain an extraordinary rich variety of biologically active peptides (Erspamer & Melchiorri, 1980; Erspamer, 1985). This has allowed the characterization of more than 50 novel peptides, including hormones, neuropeptides, and defensive peptides, often present in multiple analogous copies that may be grouped as families (Erspamer, 1983; Spindel, 1986; Bevins & Zasloff, 1990; Mor *et al.*, 1992). It is now well established that most of these amphibian peptides have either identical or closely related counterparts in mammalian brain and gastrointestinal tract. As a result of the repeated discovery of structural correspondence between amphibian skin peptides and mammalian neuropeptides or hormones, and since the skin may contain up to 100 000 times larger amounts as compared with mammalian tissues, frog skin is now considered as a model source for the discovery of new mammalian peptides and for elucidation of their biosynthetic pathways. Thus, results obtained in the study of amphibian skin peptides are of interest transcending comparative pharmacology and biochemistry as they contribute to the understanding of data assessed through investigations of mammalian counterparts. Moreover, since frog skin peptides have structural coorespondents in mammals, a careful search might uncover additional endogenous mammalian antibiotic molecules and contribute to the further illumination of our understanding of the molecular mechanisms of antimicrobial warfare.

ACKNOWLEDGMENT

This work was supported in part by funds from the CNRS and INSERM (CRE 92). The expert technical assistance of J. J. Montagne is gratefully acknowledged. We are thankful to Drs. M. Monnot and V. H. Nguyen for their help in CD spectra and antifungal assay, respectively.

REFERENCES

Bevins, C. L., & Zasloff, M. (1990) *Annu. Rev. Biochem. 59*, 395–414.

Boman, H. G., & Hultmark, D. (1987) *Annu. Rev. Microbiol. 41*, 103.

Bradbury, F. A., & Smyth, G. D. (1991) *Trends Biochem. Sci. 16*, 112.

Chen, H. C., Brown, J. H., Morell, J. L., & Huang, C. M. (1988) *FEBS Lett. 236*, 461–466.

Chung, A. L., Lear, D. J., & DeGrado, F. W. (1992) *Biochemistry 31*, 6608.

Cruciani, A. R., Barker, L. D., Zasloff, M., Chen, H. C., & Colamonici, O. (1991) *Proc. Natl. Acad. Sci. U.S.A. 88*, 3792–3796.

Csordas, A., & Michl, H. (1970) *Monatsh. Chem. 101*, 182–189.

Daly, W. J., Caceres, J., Moni, W. R., Gusovski, F., Moos, M., Seamon, B. K., Milton, K., & Myers, W. C. (1992) *Proc. Natl. Acad. Sci. U.S.A. 89*, 10960–10963.

Dayhoff, M. O., Schwartz, R. M., & Orcutt, B. C. (1978) in *Atlas of Protein Sequence and Structure* (Dayhoff, M. O., Ed.) Vol. 5, p 345, NBRF, Washington.

Dimarcq, J. L., Zachary, D., Hoffmann, J. A., Hoffmann, D., & Reichart, J. M. (1992) *EMBO J. 9*, 2507–2515.

Duclohier, H., Molle, G., & Spach, G. (1989) *Biophys. J. 56*, 1017.

Erspamer, V. (1983) *Trends Neurosci. 6*, 200–201.
Erspamer, V. (1985) *Peptides 6*, 7–12.
Erspamer, V., & Melchiorri, P. (1980) *Trends Neurosci. 1*, 391–395.
Garnier, J., Osguthorpe, D., & Robson, B. (1978) *J. Mol. Biol. 120*, 97.
Gibson, B. N., Poulter, L., Williams, D. H., & Maggio, J. E. (1986) *J. Biol. Chem. 261*, 5341–5349.
Gibson, B. N., Tang, D., Mandrell, R. K., & Spindel, E. R. (1991) *J. Biol. Chem. 266*, 23103–23111.
Giovannini, M. G., Poulter, L., Gibson, B. W., & Williams, D. H. (1987) *Biochem. J. 243*, 113–120.
Grant, E., Jr., Beeler, T. J., Taylor, K. M. P., Gable, K., & Roseman, M. A. (1992) *Biochemistry 31*, 9912–9918.
Hernandez, C., Mor, A., Dagger, F., Nicolas, P., Hernandez, A., Benedetti, L., & Dunia, L. (1992) *Eur. J. Cell Biol. 59*, 414–424.
Higgins, D. G., & Sharp, P. M. (1989) *Comput. Appl. Biosci. 5*, 151–153.
Hoffman, W., Richter, K., & Kreil, G. (1983) *EMBO J. 2*, 711–714.
Lambert, J., Keppi, I., Dimarcq, J. L., Wicker, C., Reichhart, J. M., Dunbar, B., Lepage, B., Van Dorsselaer, A., Hoffmann, J., Fothergill, J., & Hoffmann, D. (1989) *Proc. Natl. Acad. Sci. U.S.A. 86*, 262–266.
Lehrer, R. I., Ganz, T., & Selsted, E. S. (1991) *Cell 64*, 229–230.
Matsuzaki, K., Harada, M., Handa, T., Funahoshi, S., Nobutaka, F., Yajima, H., & Miyajima, K. (1989) *Biochim. Biophys. Acta 981*, 130–134.
Mor, A., & Nicolas, P. (1994) *J. Biol. Chem. 269*, 1934–1939.
Mor, A., Nguyen, V. H., Delfour, A., Migliore, D., & Nicolas, P. (1991) *Biochemistry 30*, 8824–8830.
Mor, A., Amiche, M., & Nicolas, P. (1992) *Trends Biochem. Sci. 17*, 481.
Nicolas, P., Delfour, A., Bousseta, H., Morel, A., Rholam, M., & Cohen, P. (1986) *Biochem. Biophys. Res. Commun. 140*, 565–573.
Ouellette, A. J., Greco, R. M., James, M., Frederick, D., Naftilan, J., & Fallon, J. T. (1989) *J. Cell Biol. 108*, 1687–1695.
Pouny, Y., Rapaport, D., Mor, A., Nicolas, P., & Shai, Y. (1992) *Biochemistry 31*, 12416–12423.
Rana, F. R., Macias, E. A., Sultany, C. M., Modzrakowski, M. C., & Blazyk, J. (1991) *Biochemistry 30*, 5858–5866.
Schiffer, M., & Edmundson, A. (1967) *Biophys. J. 7*, 121–135.
Segrest, J. P., De Loof, H., Dolhman, J. G., Brouillette, C. G., & Anantharamaiah, G. M. (1990) *Proteins 8*, 103–117.
Simmaco, M., Barra, D., Chiarini, F., Noviello, L., Melchiori, P., Kreil, G., & Richter, K. (1991) *Eur. J. Biochem. 199*, 217–222.
Soravia, E., Martini, G., & Zasloff, M. (1988) *FEBS Lett. 228*, 337–340.
Spindel, E. (1986) *Trends Neurosci. 9*, 130–133.
Stanfield, R. L., Westbrook, M., & Selsted, M. E. (1988) *J. Biol. Chem. 263*, 5933–5935.
Sures, I., & Crippa, M. (1984) *Proc. Natl. Acad. Sci. U.S.A. 81*, 380–384.
Terry, A. S., Poulter, L., Williams, D. H., Nutkins, J. C., Giovannini, M. G., Moore, C. H., & Gibson, B. W. (1988) *J. Biol. Chem. 263*, 5745–5751.
Wilbur, W. J., & Lipman, D. J. (1983) *Proc. Natl. Acad. Sci. U.S.A. 80*, 726–730.
Williams, R. W., Starman, R., Taylor, K. M. P., Gable, K., Beeler, T., Zasloff, M., & Covell, D. (1990) *Biochemistry 29*, 4490–4496.
Yang, J. T., Wu, C. S. C., & Martinez, H. M. (1986) *Methods Enzymol. 130*, 208–269.
Zasloff, M. (1987) *Proc. Natl. Acad. Sci. U.S.A. 84*, 5449–5453.
Zasloff, M., Martin, B., & Chen, H. C. (1988) *Proc. Natl. Acad. Sci. U.S.A. 85*, 910.